Learning accelerates the evolution of slow aging but obstructs negligible senescence

Peter Lenart[1*], Sacha Psalmon[1,2], Benjamin D. Towbin[1*]

[1]University of Bern, Institute of Cell Biology, Bern, Switzerland

[2] Polytech Nice Sophia, Côte d'Azur University, Nice, France

*to whom correspondence should be addressed

Abstract

The risk of dying tends to increase with age, but this trend is far from universal. For humans, mortality is high during infancy, declines during juvenile development, and increases during adulthood. For other species, mortality never increases, or even continuously declines with age, which has been interpreted as absent- or reverse-aging. We developed a mathematical model that suggests an alternative interpretation. The model describes the age-dependence of mortality as the sum of two opposite processes. The mortality risk due to physiological decline increases monotonously with age. But old individuals gain survival benefits through processes like growth and learning. This simple model fits mortality dynamics for all human age classes and for species across the tree of life. Simulations revealed an unexpected complexity by which learning impacts the evolution of aging. An ability to learn initially accelerated the evolution of slower aging but constrained the slowest possible rate of aging that can evolve. This constraint occurs when learning reduces mortality during the reproductive period to near negligible levels and thereby eliminates selection for a further slow-down of aging. In conclusion, learning accelerates the evolution of slower aging, but obstructs the evolution of negligible senescence for species with strong learning-associated survival benefits.

Main

Aging is frequently defined as the increase in mortality or hazard rate due to physiological decline with age[1,2]. However, mortality often does not increase monotonously with age. For example, human mortality initially declines after birth and only rises after reaching sexual maturity (Fig. 1a). For other species, such as *Hydra Magnipapillata*[3,4] or the desert tortoise *Gopherus agassizii*[5], mortality is constant across age classes or even declines with increasing age. The evolutionary mechanisms underlying this diversity in mortality dynamics are not understood.

Under the operational definition of aging as the age-dependent increase in the hazard rate[6,7], a decline in mortality with age would suggest a negative aging rate or to reverse-aging[5,8]. However, a more specific definition of aging as "age-dependent physiological decline"[1] allows for alternative interpretations. Under this definition, mortality can be a non-monotonous function of age even if physiological decline progresses continuously if age-dependent processes other than aging also impact mortality. For example, survival can be positively impacted by an increase in body mass with age. Similarly, experience from environmental interactions can provide an age-dependent survival benefit, e.g., through adaptive immunity, or through behavioral changes.

Here, we defined a mathematical model of mortality that takes these considerations into account and investigated how they impact mortality dynamics and the evolution of aging rates. We collectively refer to all survival benefits gained from experience as "learning", which explicitly includes cognitive as well as non-cognitive processes. We show that considering growth and learning allows for a quantitative description of mortality dynamics of species across the tree of life, and that learning has non-trivial implications on how aging evolves.

Survival benefits of growth and learning can account for non-monotonic mortality

Numerous mathematical models have been used to describe the relationship between age and mortality (reviewed in [9]). However, classic models struggle to mechanistically explain non-monotonicity in age-dependent mortality (Fig. 1a)[10]. Most famously, the Gomertz-Makheman model (GMM) describes the hazard rate $h_{GMM}(t)$ (the age-dependent risk of mortality) as an exponentially increasing function $h_{GMM}(t) = \alpha(t) = c + ae^{bt}$ and provides a good fit for human mortality between 30 and 80 years[11,12]. The parameter b of the GMM is called the rate of aging and represents the exponential rate increase of mortality with age.

To consider the effects of growth and learning on mortality, we developed the so-called GLA (for growth-learning-aging) model, which corrects hazard rate of the GMM $h_{GMM}(t) = \alpha(t)$ by subtracting the positive survival effects of growth $\gamma(t)$ and learning $\lambda(t)$: $h_{GLA}(t) = \alpha(t) - \gamma(t) - \lambda(t)$. We describe the survival benefits from growth $\gamma(t)$ by a decelerating function $\gamma(t) = G_{max}(1 - \frac{1}{1+t^h})$, where G_{max} is the maximal survival benefit provided by body growth. The impact of learning on survival is modeled by a logistic function $\lambda(t) = L_{max}(1 - \frac{1}{1+e^{n(t-k)}})$, where L_{max} is the maximum survival benefit provided by learning. Importantly, $\gamma(t)$ and $\lambda(t)$ describe the survival benefit stemming from growth and learning, not growth and learning themselves, and thus differ in their dynamics their respective upstream processes.

Unlike the GMM, the GLA model fits human mortality across all age classes. The GLA model captures the rapid decline at a young age, and the shoulder in the hazard rate during early maturity. Indeed, the GLA model greatly improved fits to human mortality compared to the GMM for each of the 8 countries and the 67 years that we tested (mean distance 1.21% for GLA, vs. mean distance 4.97% for GMM, Fig 1b). This improvement in fit was not explained by the larger number of parameters of the GLA model (mean Akaike information criterion: -201.6 vs. 6.15 mean AIC of GLA vs. GMM, Fig. 1c).

Fitted parameters followed consistent trends across countries and time (Fig. 1d-f, Supplemental Figure 1) that match intuitive expectations. For example, L_{max} and G_{max} (Fig. 1d-e) continuously declined between 1948 and 2015, as is expected given the great success of health care in reducing childhood mortality[13]. Also parameters that did not follow a monotonous trend, such as parameter k (Fig. 1f), showed high consistency across countries. Finally, fitted parameters matched well with general measures of population health. For example, Gmax was highly correlated to childhood mortality under 5 years (Fig. 1g), the growth exponent h was correlated with the percentage of low-weight births (Fig. 1h), and the sum of parameters c and a (corresponding to base-line mortality) closely followed life expectancy at birth (Fig. 1i).

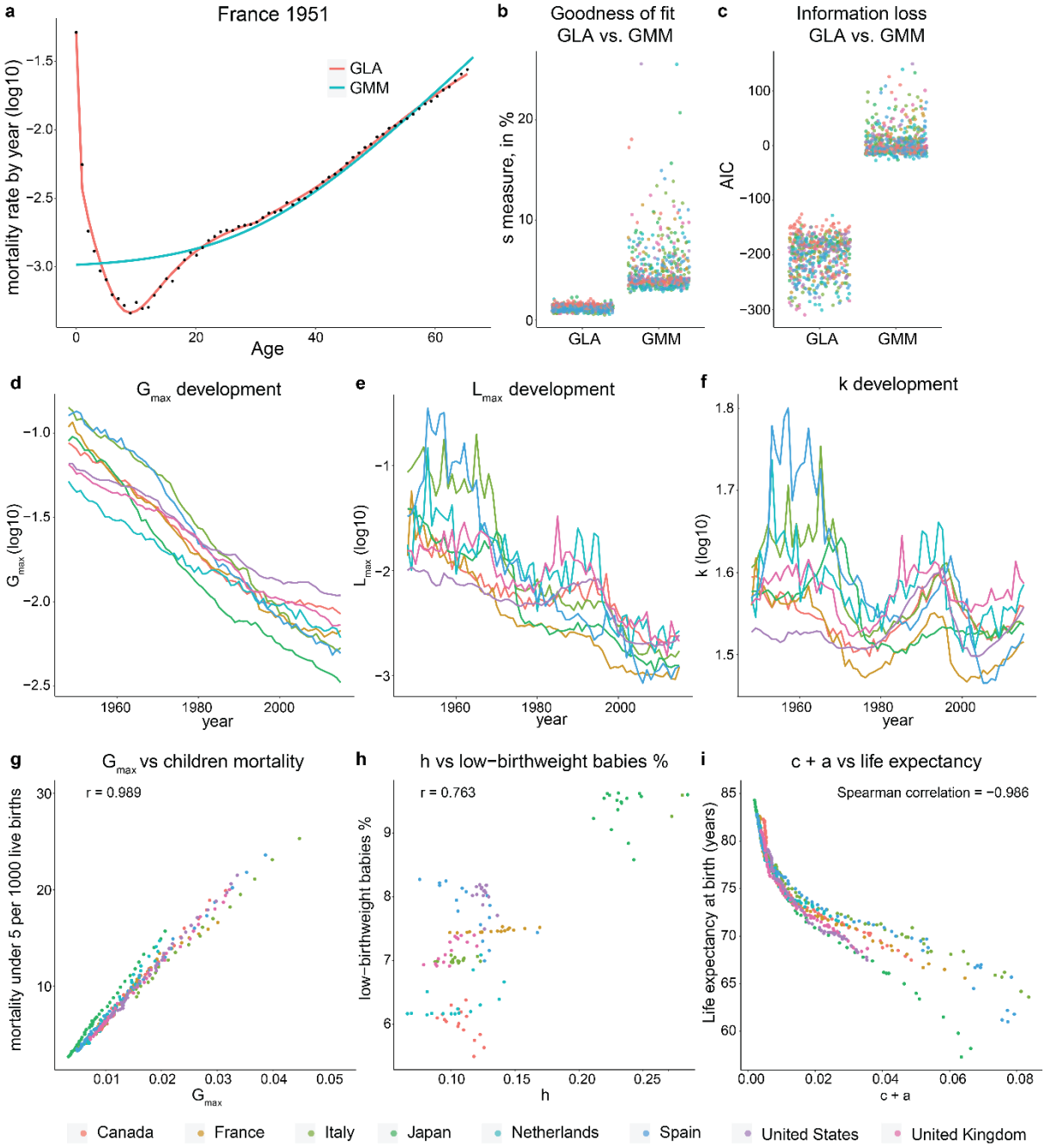

Figure 1. GLA model fits human mortality data. a. Fit of GMM (cyan) and GLA (red) models to mortality data (black circles) from France 1951 **b,c.** comparison of s measures and AIC calculated for GLA and GMM fitted to cohort mortality data (born 1948-1952), and the population data from 1948-2015 ($p < 10^{-15}$, Wilcoxon rank sum test with continuity correction). **d-f**. fitted G_{max}, k and a+c over time. **g.** correlation between % of low-birth babies[14] and value of h (growth speed) for 2000-2015, **h.** correlation of G_{max} and children mortality[14] for 1972 – 2015. **i.** correlation of c + a with life expectancy[14] for 1960 – 2015. **b-i.** color indicates countries, as indicated at the bottom of the figure.

The GLA model also generalizes beyond humans to a wide range of animal and plant species, including species with vastly different and non-monotonic mortality dynamics (Fig. 2). Although available animal and plant mortality data is less smooth due to the smaller size of the datasets [5], fits were very good overall for the GLA model. In contrast, the inherently monotonic GMM cannot fit these dynamics.

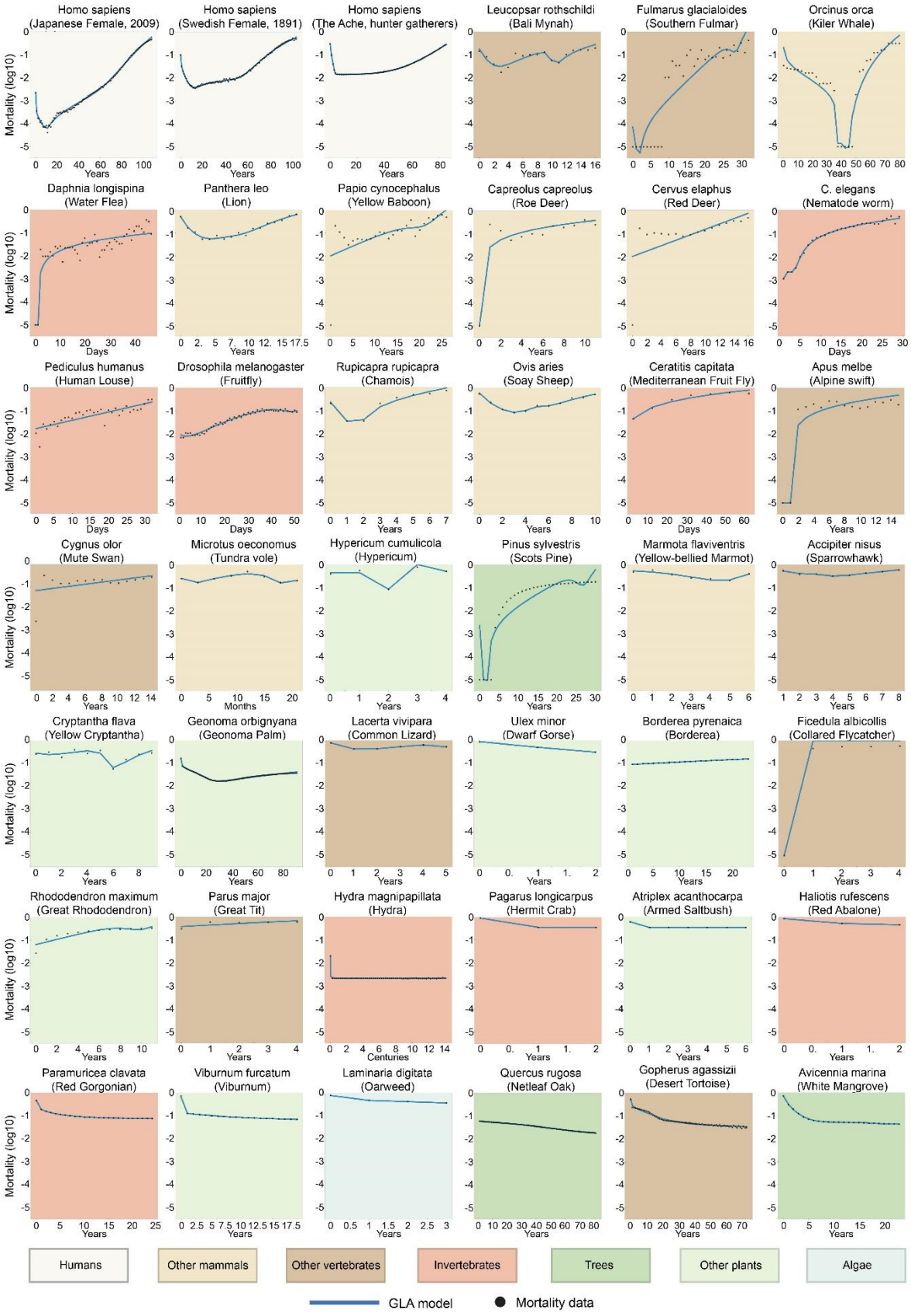

Figure 2. GLA model fits a wide variety of mortality curves across the tree of life. GLA model (red) fitted to mortality data (blue) from indicated species. The mortality curves are ordered as in the source of mortality data[5] based on their overall trend. Top left: Species in

which mortality increases with age, bottom right: species for which mortality declines with age. Data is shown from birth to the age when 5% of the adult population remains alive.

Learning non-monotonically impacts the evolution of aging

By distinguishing the influence of aging and learning on mortality, the GLA model allowed us to ask how learning affects the evolution of aging. To this end, we used agent-based simulations, where individual agents underwent repeated rounds of reproduction, mortality, and mutation. Briefly, we initiated simulations with 10'000 individuals using parameters obtained from fits of the GLA model to human data. Individuals reproduced at an age-dependent rate determined by a Brass polynomial which closely matches reproduction of humans[15]. The mortality rate of each individual was determined by the GLA model, and each individual was given a 2% chance of mutation to in- or decrease the rate of aging (parameter b in the GLA model). Whereas this evolutionary model did not consider tradeoffs between aging and other life-history traits, we show in the supplemental information that our overall conclusions are robust to including such tradeoffs (Supplemental Figure 2).

As expected, during early time points of the simulation, the aging rate rapidly declined (Fig. 3a). However, at longer time scales, the slow-down of aging decelerated and plateaued (Fig. 3b). An ability to learn non-trivially impacted how quickly the aging rate evolved. The initial decline in the aging rate (b) was faster for simulatons with a stronger effect of learning on surivival (L_{max}) (Fig. 3a, c). However, learning had the opposite effect on the plateau and increased the slowest rate of aging that evolved at long time scales (Fig. 3b, d). These data suggest an unexpected complexity in the relation between the evolution of learning and aging: learning accelerated the evolution of slower aging initially but constrained the lowest rate of aging that can evolve.

Simulations of where L_{max} and b were allowed to co-evolve were consistent with these results. L_{max} increased slightly during the evolution, and the final rate of aging was thus further

increased (Fig. 3b). A similar pattern also emerged from simulations of asexual populations with constant reproduction, although in this case, the aging rate b never reached a complete plateau (Supplemental Figure 3).

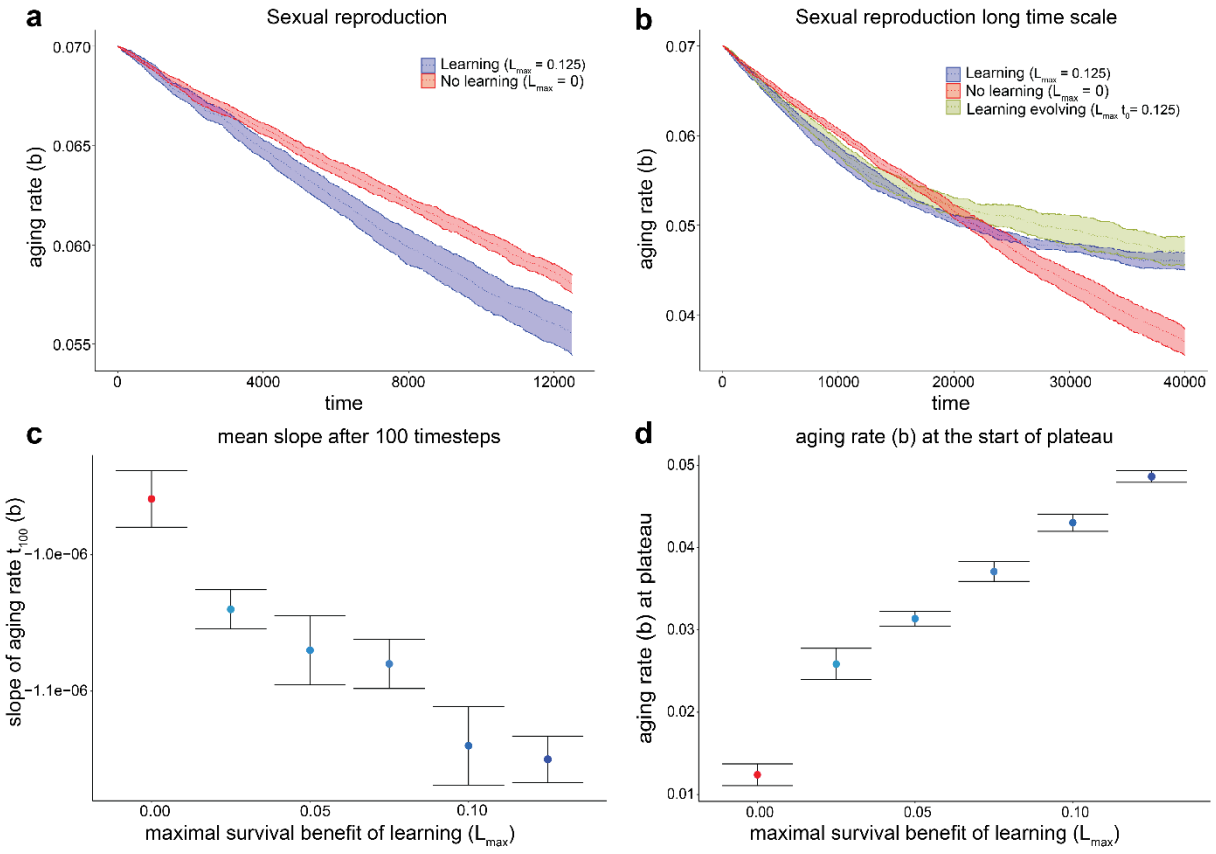

Figure 3. Learning accelerates the evolution of slower aging in agent-based simulations and increases the lowest rate of aging that can evolve. a. Evolution of aging rate in the simulation of sexually reproducing organisms with fertility and mortality parameters taken from fits to human data. A Brass polynomial was used to model a fertility function matching human data based on ref [15]. Other life history parameters were taken from fits of the GLA model to morality data from France 1951. **b**. as a, but for longer time scales and additionally showing the results of a simulation where aging and learning co-evolved. For co-evolution, L_{max} was 0.125 at the beginning of the simulations and then allowed to evolve. **c.** Mean +/- SEM of the slope of aging rate evolution during the first 100 timesteps (n = 625 independent simulations with m = 10'000 individuals). **d.** Mean +/- SD of aging rate at the point at which evolution of slower aging decelerated (n = 10 independent simulations with m = 10'000 individuals)

Low mortality during reproduction due to learning weakens selection of slower aging

To understand why the impact of learning on the evolution of aging inverts at low aging rates, we used deterministic simulations to compute selective fitness over a wide range of L_{max} and b. Specifically, we calculated fitness as the intrinsic rate of population increase r by the Euler-Lotka equation[16] from the same model as used above (Fig. 4a). We then determined the selection strength for slower aging, as the change in fitness resulting from a 1% reduction in the rate of aging b (Fig. 4b). From this, we calculated the difference in the selection strength in the presence and absence of learning (Fig. 4c). Fig. 4 shows simulations for parameters obtained from 1951 population data of France.

For a wide range of parameters, including those matching human mortality data from all 8 countries and 67 years tested, the fitness benefit of slower aging increased with a higher degree of learning ($\frac{\partial r}{\partial L_{max} \partial b} > 0$ for all countries, France 1951 shown in Fig. 4b) . Thus, humans are in a parameter space where, learning accelerates the evolution of slower aging, consistent with results from agent-based simulations (Fig. 3). The shape of the fitness landscape was qualitatively robust to the choice of the fertility function, producing equivalent conclusions for decreasing, constant, and increasing fertility with age (Supplemental Figure 4).

The lower right corner of the fitness landscape (high $L_{max,}$ low b) shows a plateau where a slow-down of aging has no further effect on fitness (Fig. 4b). Indeed, mapping the trajectories from agent-based simulations onto the fitness landscape shows that evolution loses directionality once the fitness plateau is reached (Fig. 4c). Thus, the edge of the plateau indicates the slowest rate of aging that is selected. Notably, the shape of the plateau is such that this lower bound of the selectable aging rates increases with L_{max} (Fig. 4c), consistent with results from agent-based simulations (Fig. 3d).

An intuitive explanation for the fitness plateau and its shape is revealed by inspection of the reproductive output along the evolutionary trajectories. When the aging rate drops below a threshold b_T where mortality becomes negligible during the reproductive period, a further reduction in the aging rate does not increase reproductive output (Fig. 4d, e). Hence, there is no selective pressure for rates of aging below b_T. This threshold b_T occurs already at a higher rate of aging when mortality is additional suppressed by learning. Together, our analysis explains the seemingly paradoxical impact of learning on the speed at which aging slows-down during evolution (Fig 4e).

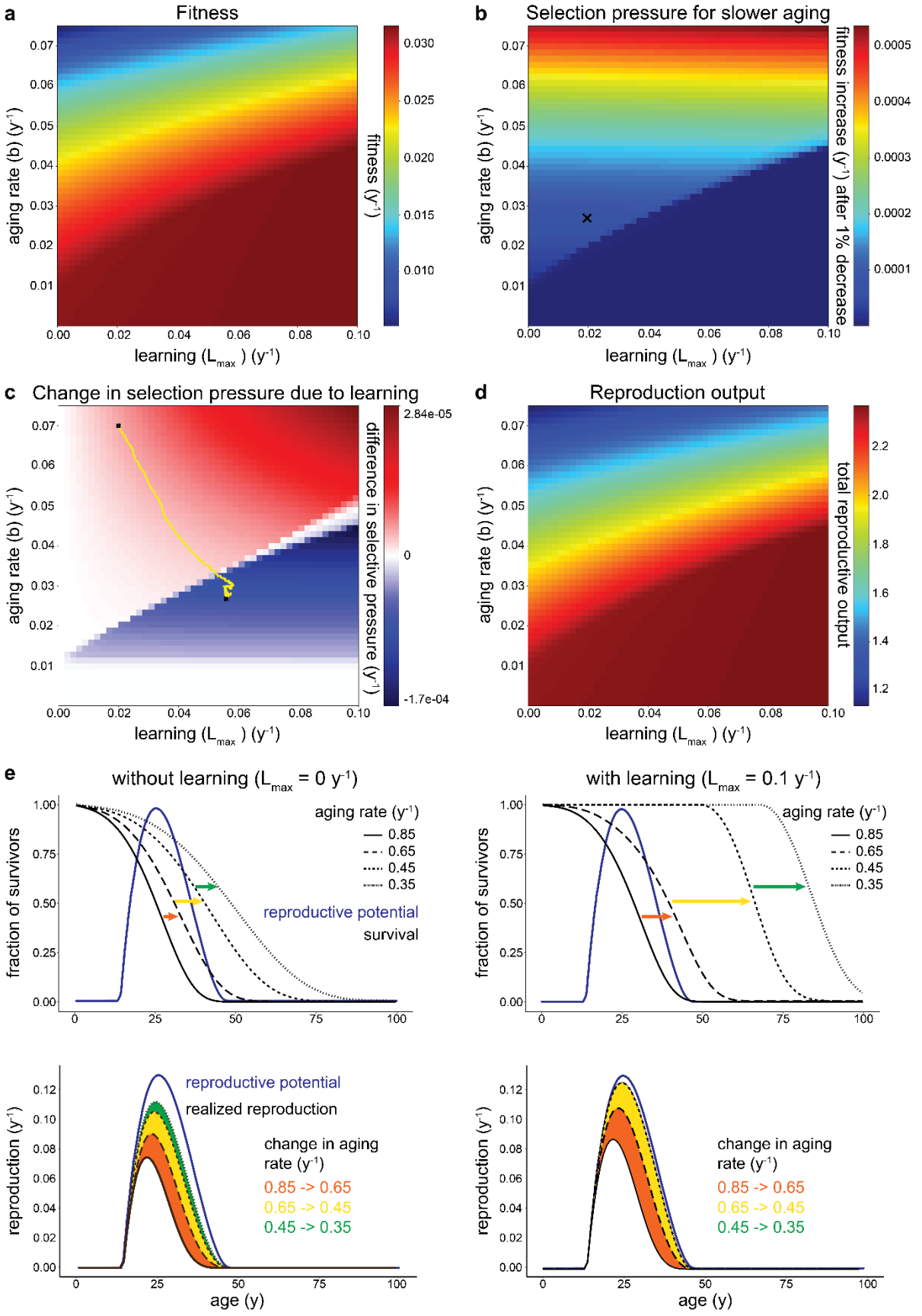

Figure 4 Fitness landscape distinguishes regions where learning accelerates or constrains the evolution of slower aging. a. absolute fitness as a function of the maximal benefit of learning (L_{max}) and the rate of aging (b). **b**. selective pressure for slower aging as a function of

the maximal benefit of learning and the rate of aging . Selective pressure was calculated as the absolute fitness benefit in intrinsic rate of population increase (r) from a 1% reduction in the rate of aging. Black cross marks location of fitted parameters for France 1951. **c**. as (**b**), but relative to the selective pressure in the absence of learning ($L_{max} = 0$). Red color indicates the parameter space where learning accelerates the evolution of slower aging. yellow line: agent-based simulation of sexual reproduction and co-evolution of learning and aging for 120 000 timesteps (average trajectory of 10 independent simulations with 10 000 individuals each). Black crosses:starting and end values of the simulation. **d**. Reproductive output (total number of offspring produced per individual) as a function of L_{max} and b. **e.** Graphical illustration of the interaction between learning and the evolution of aging. Initially, the same decrease in aging rate without learning (left) leads to smaller increase of reproductive output than with learning (right). However, at some point mortality during reproductive period becomes negligible with learning but not without it which reverses the situation.

Discussion

We developed the GLA model, which integrates the effects of aging, learning, and growth on mortality, and thereby provides good fits to mortality data across the tree of life. The model distinguishes between age-dependent processes that increase mortality, which we call aging, and those that reduce mortality, which we summarize as growth and learning.

We used the GLA model to analyze learning impacts the evolution of aging. We find that an ability to learn initially accelerates the evolution of slower aging, which is in good agreement with observational data. Brain size of birds and mammals correlates with their maximum longevity[17–20, 21] and zoo records of parrots support a direct relationship between larger brains and longer life expectancy[22]. Previous theories, such as the *cognitive buffer hypothesis*[17], have explained this relation by the reduction of extrinsic mortality due to a bigger cognitive flexibility. Our model suggests that learning additionally favors slower physiological aging on an evolutionary timescale, consistent with previous theoretical work on phenotypic plasticity [23].

Additionally, we reveal scenarios under which learning sets a lower bound on aging rates, namely when learning reduces the mortality rate during the reproductive period to near negligible levels. The GLA model thus predicts that only species with no or little survival

benefits from learning can evolve negligible senescence. Indeed, most organisms with negligible senescence, such as hydra[3–5], do not show obvious signs of coginitive learning or other experienced-based survival benefits, such as adaptive immunity [24]. Notably, this includes more than 90% of angiosperms [25–27].

ur conclusions are compatible, but independent of, classical theories on the evolution of aging. Mutation-accumulation theory[28] and the hypothesis of antagonistic pleiotropy[29] suggested a selection shadow, where aging evolved because the strength of selection declines with age due to the decreasing pool of survivors. In the GLA model, learning dampens this selection shadow by reducing mortality at a young age, and consistently increases the selection for slow-down of aging (Fig. 3). The disposable soma theory[30] proposes a tradeoff between somatic maintenance and reproduction. The survival benefits of learning ultimately depend on the correct function of somatic tissues (e.g., brains, sensory organs, immune system). Somatic maintenance is therefore required for effective learning, and vice-versa learning could increase the fitness benefit of somatic maintenance. For example, it is conceivable that effective learning positively affects mating success. This positive feedback may further accelerate the evolution of slower aging.

Together, we have shown that the effects of growth and learning can explain the diversity of age-dependent mortality dynamics across the tree of life, and that an ability to learn impacts the evolution of aging. Separating age-related effects on mortality into beneficial and detrimental processes is compatible with conventional theories of aging and makes an important contribution to explaining why negligible senescence occurs in some species, but not in others.

Methods

General model

The GLA model describes the hazard rate $h(t)$ as the sum of effects of aging (α), growth (γ) and learning (λ) on survival, each of which has a distinct time dependence:

$$h(t) = \alpha(t) - \lambda(t) - \gamma(t)$$

aging follows the Gompertz-Makeham function[9], a commonly used model of aging:

$$\alpha(t) = c + ae^{bt}$$

c, a, and b are constant parameters, and t represents time. The parameter b is called the aging rate, the exponential rate at which mortality due to aging increases with time.

Learning reduces mortality with age by a logistic function which plateaus to a maximal benefit of learning L_{max}:

$$\lambda(t) = L_{max}(1 - \frac{1}{1 + e^{n(t-k)}})$$

k is the age at which the benefits of learning reach half their maximum. n determines the steepness of the learning curve.

We modeled the benefits of growth by a deaccelerating function.

$$\gamma(t) = G_{max}(1 - \frac{1}{1 + t^{h}})$$

G_{max} corresponds to the maximal survival benefit due to growth and h relates to the growth speed. Supplemental Figure 5 illustrates the shapes of those three functions. Importantly, our conclusions are robust to details of the model implementation, for example, using different functions to model aging (Supplemental Figure 6).

Mortality data

Data on human mortality rates were acquired from the human mortality database[31] on 20 April 2022. We have analyzed the birth cohort (longitudinal) and population data (cross-sectional). Analysis was restricted to mortality data after 1948. Cohort data of at least 65 years were available for 26 countries. We focused on the 8 countries with a population of over 10 million in 1948. Population data was taken from 1948 to 2015 for the same countries. Animal and plant mortality data are from ref [5], excluding six species (*Agave marmorata*, *Rana Aurora*, *Macrotrachela quadricornifera*, *Crocodylus johnsoni*, *Pan troglodytes* and *Poecillia reticulata*) due to sparse or short data.

Fitting the GLA model

SLSQP (implemented in the scipy.optimize Python package)[32], and CMA-ES (implemented in the CMA Python package)[33] were used to fit the parameters of the GLA model to log transformed mortatlity data. Out of two fits, we always chose the better one assessed by the standard error of the regression, further referred to S measure). For fitting human data, a constraint was set for growth and its associated benefits to stop changing at age 30 since at this point, all growth and development is completed [34].

Computation of fitness functions and the benefit of slower aging

We used the intrinsic rate of population increase r as a measure of Darwinian fitness, defined by the Euler-Lotka equation[16]

$$\sum_{x=0}^{\infty} e^{-rx} l_x m_x = 1$$

l_x is the likelihood of survival to age x. m_x corresponds to the number of offspring produced by individuals of age x. Based on the GLA model, survivorship l_x was calculated as:

$$l_x = 1 - \int_{t=0}^{x} \big(\alpha(t) - \lambda(t) - \gamma(t)\big)\, dt$$

For m_x we used a Brass Polynomial defined as

$$m_x(c,d,w) = \begin{cases} c(x-d)(d+w-x)^2 & if\ (d+w) > x > d \\ 0 & otherwise \end{cases}$$

For models shown in in Supplemental data, we used constant ($m_x = c$), increasing ($m_x = b_0(1 + (0.05x))$), or decreasing ($m_x = \frac{b_0}{1+(0.05x)}$) functions.

Fitness landscapes in Figure 4 were based on parameters form fitting to French population mortality data from 1951. Fitness landscapes produced using parameters from other countries and years were very similar.

Agent-based models

For all agent-based simulations, time was discrete, with each time step corresponding to the age increment of 1 and with all relevant rates and probabilities defined on a per-time step basis. Each simulation was run in 10 replicates unless stated otherwise in the main text. Parameters were taken from fits to French population mortality from 1951. Conclusions were robust to using parameters from fits to cohort or population form data from other countries and years.

Asexual agent-based model

Each agent was represented by three characteristics: its age x, its aging rate b, and its maximum benefit of learning L_{max}. At the start of the simulation, 20’000 agents were assigned an age x drawn from a normal distribution with mean 30 and standard deviation (SD) 10, and a rate of aging b from a normal distribution with mean = 0.15 and SD = 0.001. L_{max} was constant for all individuals. In each time-step, the chance of dying *h* was calculated for each individual and survival was determined by a Bernoulli trial. Surviving individuals were then picked at random

and cloned until the population reached 20'000 individuals. Cloned individuals had an age of 1 and otherwise the same parameters as their parents. For each newly born agent there as a 2% chance of mutation in the aging parameter b where a new parameter b was drawn from a normal distribution centered around the pre-mutation value with SD of 0.0075. For a summary of parameters, see Supplemental Table 1. Simulations were run using statistical software R (v. 4.2.0.)

Sexual model

Each agent was represented by four attributes: its sex, its age x, its aging rate b, and its maximum benefit of learning L_{max}. When initializing the simulation, each agent was assigned x and b drawn from a normal distribution (mean(x) = 30, SD(x) = 10; mean (b) = 0.07, SD (b) = 0.001). L_{max} was constant for all individuals. The initial population size was set to 5'000 and the maximum population size was capped at 10'000. Starting simulations with a population size of 10'000 did not affect the conclusions (Supplemental Figure 7).

For every round of the simulation, the probability of death was computed based on the GLA model for each agent. Survivorship was determined by a Bernoulli trial, followed by either increasing the age by 1 or removing the agent from the simulation.

Reproduction was modeled by the Brass Polynomial as described above using parameters obtained from human fertility data of men and women[15]. To optimize computations, simulations were discontinued for agents whose age was above the fertile period ($w + d$). Simulations where post-reproductive individuals were not removed led to identical consclusions (Supplemental Figure 7). The probability p of an agent to reproduce in a given round was calculated by:

$$p_x(c, d, w) = \frac{m_x(c, d, w)}{\max\left(m_x(c, d, w)\right)}$$

All agents were then randomly paired as male and female couples. If both agents of a couple were able to reproduce, they produced a new agent of random sex. The aging rate b of the new agent was assigne the mean b of its parents. 2% of all newly created agents were then randomly selected to mutate and assigned an aging rate b drawn from a normal distribution with mean being its pre-mutation value and SD = 0.006.

Parameters used in the simulations are summarized in Supplemental Table 1. Simulations were run using Python version 3.8.10.

Aging rate plateau

The aging rate plateau in Figure 3d was operationally defined as the time point the aging rate changed by less than 0.5% of the initial aging rate within 1'250 time steps. Specifically, we calculated the mean aging rate in two consecutive windows of 1'250 time steps and calculated the difference between these means. A plateau was called when this difference was twice in a row lower than 0.5% of the initial aging rate.

Acknowledgments

We thank Claudia Bank, Luděk Berec, Thomas Flatt and Omer Karin for helpful discussions and comments on a draft of the manuscript. P.L. was funded by the SNSF Swiss Postdoctoral Fellowships (TMPFP3_209681). This work received funding from the Swiss National Science Foundation (SNSF) in the form of an Eccellenza Professorial Fellowship (PCEFP3_181204) to B.D.T.

Authors contributions:

PL formulated the research problem, created the model, designed and ran the agent-based simulations, executed fitness function computations, and wrote the manuscript. SP, improved the model and algorithms for fitting, computation of fitness landscapes, and agent-based simulations and co-wrote the manuscript. BT supervised the project and edited the manuscript.

Competing interests

The authors declare no competing interests

Supplementary Information

Supplementary Information is available for this paper

Code availability

Code used for this study is available at

https://github.com/PeterLenart/Learning_accelerates_aging.git

References:

1. Flatt, T. A New Definition of Aging? *Front. Genet.* **3**, 148 (2012).
2. Kirkwood, T. B. L. & Austad, S. N. Why do we age? *Nature* **408**, 233–238 (2000).
3. Schaible, R. *et al.* Constant mortality and fertility over age in Hydra. *Proc. Natl. Acad. Sci.* **112**, 15701–15706 (2015).
4. Martínez, D. E. Mortality patterns suggest lack of senescence in hydra. *Exp. Gerontol.* **33**, 217–225 (1998).
5. Jones, O. R. *et al.* Diversity of ageing across the tree of life. *Nature* **505**, 169–173 (2014).
6. Pedro de Magalhães, J. *et al.* A Reassessment of Genes Modulating Aging in Mice Using Demographic Measurements of the Rate of Aging. *Genetics* **208**, 1617–1630 (2018).
7. Finch, C. E., Pike, M. C. & Witten, M. Slow mortality rate accelerations during aging in some animals approximate that of humans. *Science* **249**, 902–905 (1990).
8. W. Vaupel, J., Baudisch, A., Dölling, M., A. Roach, D. & Gampe, J. The case for negative senescence. *Theor. Popul. Biol.* **65**, 339–351 (2004).
9. Pham, H. Mortality Modeling Perspectives. in *Recent Advances in Reliability and Quality in Design* (ed. Pham, H.) 509–516 (Springer, 2008). doi:10.1007/978-1-84800-113-8_25.
10. Avraam, D., de Magalhaes, J. P. & Vasiev, B. A mathematical model of mortality dynamics across the lifespan combining heterogeneity and stochastic effects. *Exp. Gerontol.* **48**, 801–811 (2013).
11. Easton, D. M. & Hirsch, H. R. For prediction of elder survival by a Gompertz model, number dead is preferable to number alive. *Age* **30**, 311–317 (2008).
12. Nash, F. *Reliability Assessments : Concepts, Models, and Case Studies*. (CRC Press, 2017). doi:10.1201/9781315371009.
13. Roser, M., Ritchie, H. & Dadonaite, B. Child and Infant Mortality. *Our World Data* (2013).

14. World Development Indicators | DataBank. https://databank.worldbank.org/.

15. Gage, T. B. Age-specific fecundity of mammalian populations: A test of three mathematical models. *Zoo Biol.* **20**, 487–499 (2001).

16. Baudisch, A. Hamilton's indicators of the force of selection. *Proc. Natl. Acad. Sci.* **102**, 8263–8268 (2005).

17. Allman, J., McLaughlin, T. & Hakeem, A. Brain weight and life-span in primate species. *Proc. Natl. Acad. Sci. U. S. A.* **90**, 118–122 (1993).

18. Hofman, M. A. Encephalization and the evolution of longevity in mammals. *J. Evol. Biol.* **6**, 209–227 (1993).

19. González-Lagos, C., Sol, D. & Reader, S. M. Large-brained mammals live longer. *J. Evol. Biol.* **23**, 1064–1074 (2010).

20. Minias, P. & Podlaszczuk, P. Longevity is associated with relative brain size in birds. *Ecol. Evol.* **7**, 3558–3566 (2017).

21. Jiménez-Ortega, D., Kolm, N., Immler, S., Maklakov, A. A. & Gonzalez-Voyer, A. Long life evolves in large-brained bird lineages*. *Evolution* **74**, 2617–2628 (2020).

22. Smeele, S. Q. *et al.* Coevolution of relative brain size and life expectancy in parrots. *Proc. R. Soc. B Biol. Sci.* **289**, 20212397 (2022).

23. Paenke, I., Sendhoff, B., Kawecki, T. J., Gomulkiewicz, A. E. R. & Whitlock, E. M. C. Influence of Plasticity and Learning on Evolution under Directional Selection. *Am. Nat.* **170**, E47–E58 (2007).

24. Deines, P., Lachnit, T. & Bosch, T. C. G. Competing forces maintain the Hydra metaorganism. *Immunol. Rev.* **279**, 123–136 (2017).

25. Salguero-Gómez, R., Shefferson, R. P. & Hutchings, M. J. Plants do not count… or do they? New perspectives on the universality of senescence. *J. Ecol.* **101**, 545–554 (2013).

26. Baudisch, A. *et al.* The pace and shape of senescence in angiosperms. *J. Ecol.* **101**, 596–606 (2013).

27. Han, G.-Z. Origin and evolution of the plant immune system. *New Phytol.* **222**, 70–83 (2019).

28. Medawar, P. B. *An Unsolved Problem of Biology: An Inaugural Lecture Delivered at University College, London, 6 December, 1951*. (H.K. Lewis and Company, 1952).

29. Williams, G. C. Pleiotropy, Natural Selection, and the Evolution of Senescence. *Evolution* **11**, 398–411 (1957).

30. Kirkwood, T. B. L. Evolution of ageing. *Nature* **270**, 301–304 (1977).

31. HMD. Human Mortality Database. Max Planck Institute for Demographic Research (Germany), University of California, Berkeley (USA), and French Institute for Demographic Studies (France). https://www.mortality.org/.

32. Virtanen, P. *et al.* SciPy 1.0: fundamental algorithms for scientific computing in Python. *Nat. Methods* **17**, 261–272 (2020).

33. Hansen, N. cma: CMA-ES, Covariance Matrix Adaptation Evolution Strategy for non-linear numerical optimization in Python.

34. Volpi, E., Nazemi, R. & Fujita, S. Muscle tissue changes with aging. *Curr. Opin. Clin. Nutr. Metab. Care* **7**, 405–410 (2004).